Indian Journal of Pure & Applied Physics
Vol. 63, June 2025, pp. 488-496
DOI: 10.56042/ijpap.v63i6.15435

Miniaturized Metamaterial Loaded Multiband Antenna for Sub-6 GHz Applications

Anusha K[1*] & Mohana Geetha D[2]

[1] Department of Electronics and Communication Engineering, Kumaraguru College of Technology, Coimbatore 641 049, India

[2] Department of Electronics and Communication Engineering, Sri Krishna College of Engineering and Technology, Coimbatore 641 008, India

Received: 1 December 2024; accepted: 15 May 2025

A multiband metamaterial loaded antenna of dimensions 37.5 × 45 mm^2 is designed to resonate at four frequencies 1.74, 2.48, 3, and 3.5 GHz respectively suitable for sub-6 GHz applications. The initial structure incorporates slots to facilitate multiband capabilities. The slot dimensions in the radiating patch are determined through parametric analysis. Further, Genetic Algorithm (GA) and Quasi Newton (QN) optimization are utilized to validate the results of parametric analysis. For miniaturization, the Split Ring Resonator (SRR) and Complementary Split Ring Resonator (CSRR) are incorporated and analyzed. The inclusion of a metamaterial unit cell resulted in a size reduction of 53% from the conventional structure. Along with size reduction, there is a substantial improvement in gain for CSRR incorporated structure. The proposed CSRR implemented structure has been fabricated and the validation of the results is carried out.

Keywords: CSRR, Genetic algorithm, Quasi-Newton method, WLAN, WiMAX

1 Introduction

Great progress has been observed in recent times for antennas having lightweight, superior performance, and multiband operation in wireless communication technology. A multiband antenna transmits and receives signals at multiple frequencies making this more advantageous than a single-band antenna[1]. The multiband antenna can be materialized by the inclusion of slots, notching, or variation in the patch structure[2]. Multiple techniques widely employed to improve the antenna performance like the inclusion of slots, defected ground, and frequency selective surfaces[3].

In recent times the incorporation of metamaterials in the radiating structure has improved the performance of the antenna. Metamaterials are artificial structures that possess unique properties enabling effects that cannot be realized in natural existing materials[4]. Applying metamaterial in the antenna structure provides many advantages such as enhancing gain, increasing bandwidth, and significantly reducing the dimensions of the antenna. Implementation of metamaterial properties in the antenna structure is done by using unit cells[5]. There are two types of unit cells SRR and CSRR structure. The unit cell inclusion in the radiating structure improves the performance of the resonating frequencies obtained from the multiband antenna[6,7].

There are various algorithms available to perform the optimization of the antenna parameters[8,9]. GA optimizer represents a technique utilized to address arbitrary variables by executing additional iterations, resulting in increased time consumption. GA allows for the manipulation of a greater number of variables. The cost function reaches zero at a certain variable. A QN optimizer is an approach used to solve data within gradient searches. Its main aim is to minimize or maximize the value of the design parameter. One or two variables can be changed in the QN optimizer to attain the cost value of zero. Variation of more than two variables is not possible in this optimizer. The cost function relates to the variable in the model and attains the goal value given.

A hexagonal triband antenna operating in S, C, and X bands is proposed with rectangular and circular slots[10]. The slots aid in achieving multiband operation with appreciable gain values. In[11] a compact antenna on a FR4 substrate with single resonance at 3.5 GHz is realized using CSRR in the ground and slots in the

*Corresponding author: (E-mail: anusha.k.ece@kct.ac.in)

patch. The structure has a gain of 3dBi and a bandwidth of 200 MHz. A dual band antenna on FR4 substrate with a compact size is designed using a fractal monopole with rectangular slots for WiMAX applications[12]. A quad band antenna suitable for wireless applications is designed with a tapered patch and CSRR[13]. Multiple CSRRs are etched in the modified patch to improve the gain of the antenna. The loading of CSRR in the ground plane results in gain enhancement improving the radiation characteristics[14].A combination of circular and hexagonal unit cell as a meta surface layer is utilized to improve the gain of the antenna[15]. A triband antenna with SRR array is designed suitable for wireless applications[16].

In the existing works, the dimensions of the multiband antenna are larger making it impractical to be deployed for wireless applications. Besides, it is challenging to ensure optimal gain in a miniaturized multiband antenna. The proposed work aims to address these challenges by incorporating metamaterials. The proposed antenna achieves 53% miniaturization along with enhanced gain. The significant contributions of this research article are stated below:

- Proposed a miniaturized multiband microstrip antenna design utilizing metamaterial structures and optimization algorithms.
- Incorporated an 'E' shaped slot near the feed point to achieve resonance at multiple bands, enhancing the antenna's frequency versatility.
- Conducted parametric analysis to determine the dimensions of slots, optimizing them for resonance at multiple frequencies. Utilized GA and QN methods for antenna dimension optimization to validate the same.
- Designed and analyzed the metamaterial unit cells to achieve negative permittivity and permeability in the operating frequency range.
- Incorporated metamaterial structure and achieved significant enhancements in antenna gain and miniaturization compared to conventional and existing designs, with improved radiation characteristics across multiple operating frequencies.
- Validated the simulated results through measurements in an anechoic chamber, demonstrating the antenna's effectiveness in achieving resonance at multiple frequencies with low return loss and improved gain characteristics.

2 Antenna Design Methodology

The proposed design aims to achieve a miniaturized multiband microstrip antenna by incorporating metamaterial structures and optimization algorithms. FR4 epoxy material is used as a substrate with a dielectric constant of 4.4. The height of the substrate (h) is 1.6 mm. The simulations are carried out in Ansys High Frequency Simulation Software (HFSS-Finite Element Method).

2.1 Conventional Rectangular Patch Antenna

Initially, a conventional rectangular patch antenna of size 60 mm × 60 mm is designed for a resonating frequency of 2.3 GHz. Various parameters like patch width, effective dielectric constant ϵ_{reff}, and patch length L are determined using Eq (1- 4)[17]

$$\text{Width of the patch, W} = \frac{C_o}{2f_r}\sqrt{\frac{2}{\epsilon_r+1}} \quad \ldots (1)$$

$$\in_{reff} = \left[\frac{\varepsilon_r+1}{2} + \frac{\varepsilon_r-1}{2}\right]\left[1+12\frac{h}{w}\right]^{-1/2} \quad \ldots (2)$$

$$\text{Patch Extension Length } (\Delta L) = \frac{h\times 0.412\,(\epsilon_{reff}+0.3)\left(\frac{w}{h}+0.264\right)}{(\epsilon_{reff}-0.258)\left(\frac{w}{h}+0.8\right)}. \quad \ldots (3)$$

$$\text{Length of the Patch, L} = \frac{C}{2f_0\sqrt{\epsilon_{reff}}} - 2\Delta L \quad \ldots (4)$$

Where C_0 denotes the speed of light and its value is 3 x 10^8 m/s, f_r represents resonating frequency, ε_{reff} is the effective dielectric constant and ε_r indicates relative dielectric constant. The dimensions of the radiating patch's ground plane are estimated using Eq (5) and Eq (6).

$$L_g = 6h + L \quad \ldots (5)$$

$$W_g = 6h + W \quad \ldots (6)$$

The conventional antenna designed as in Fig. 1 (a) offers resonance at 2.3 GHz. At this frequency, the magnitude of S_{11} is observed as -12.28 dB and the simulated gain is observed as 3.1 dB.

2.2 Multiband E-Slotted Rectangular Patch Antenna

The performance of an antenna is determined by its dimensions, including width, length, and height. Suboptimal patch width can lead to poor antenna performance, characterized by high return loss and low gain. GA and QN methods are employed to arrive at the optimal patch width of the radiating structure. The objective function for both algorithms is return

loss reduction and gain enhancement. GA serves as an approach to narrow down the search space and QN optimizer is utilized to resolve data within gradient searches. In general, the optimization process is initiated with a parametric setup. GA takes random values whereas for Quasi Newton input should be given manually.

For GA the width of the patch varies from 30 mm to 45 mm. The GA optimization values are taken randomly in the given range. The cost is lower at 35.70 mm, 35.66 mm, and 35.65 mm. With the results of the GA algorithm, the input range of the QN optimizer search space is refined to 34 mm to 38 mm.

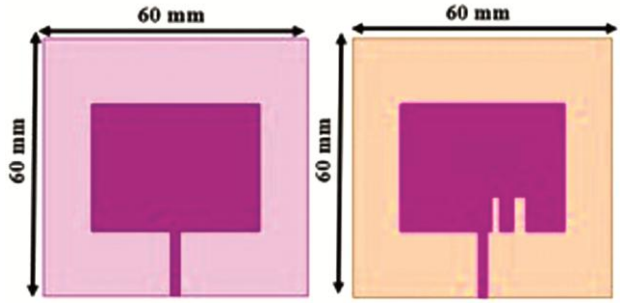

Fig. 1 — Antenna structure (a) Conventional Rectangular Patch, and (b) Slotted Multiband Patch Antenna

Five values of patch dimensions have been given as an input range. The cost values at 34 mm, 35 mm, 36 mm, 37 mm, and 38 mm are 238.4, 156.37, 146.72, 218.79 and 253.22 respectively. The optimal width of the patch antenna is identified as 36 mm, where the lowest cost function is achieved. Both algorithms converge to the same optimized width of 36 mm. Further, to attain resonance at multiple bands in the optimized structure, an 'E' shaped slot has been included near the feed point. The optimized multiband radiating structure is depicted in Fig. 1 (b).

The position of the slots is determined from the current distribution. The dimensions of the slots are finalized through parametric analysis. For parametric analysis, the length and width of the slots are considered. First, a single rectangular slot is placed near the slot. The length of the first slot (L_1) varied from 4 mm to 12 mm with a step size of 2 mm. The width of the first slot (W_1) varied from 0.5 mm to 3.5 mm with a step size of 0.5 mm.

From the result of the parametric analysis as in Fig. 2 (a), it is observed that the antenna resonates at three different frequency bands with acceptable performance for L_1 = 8 mm and W_1 = 2 mm. To achieve additional resonance, another rectangular slot

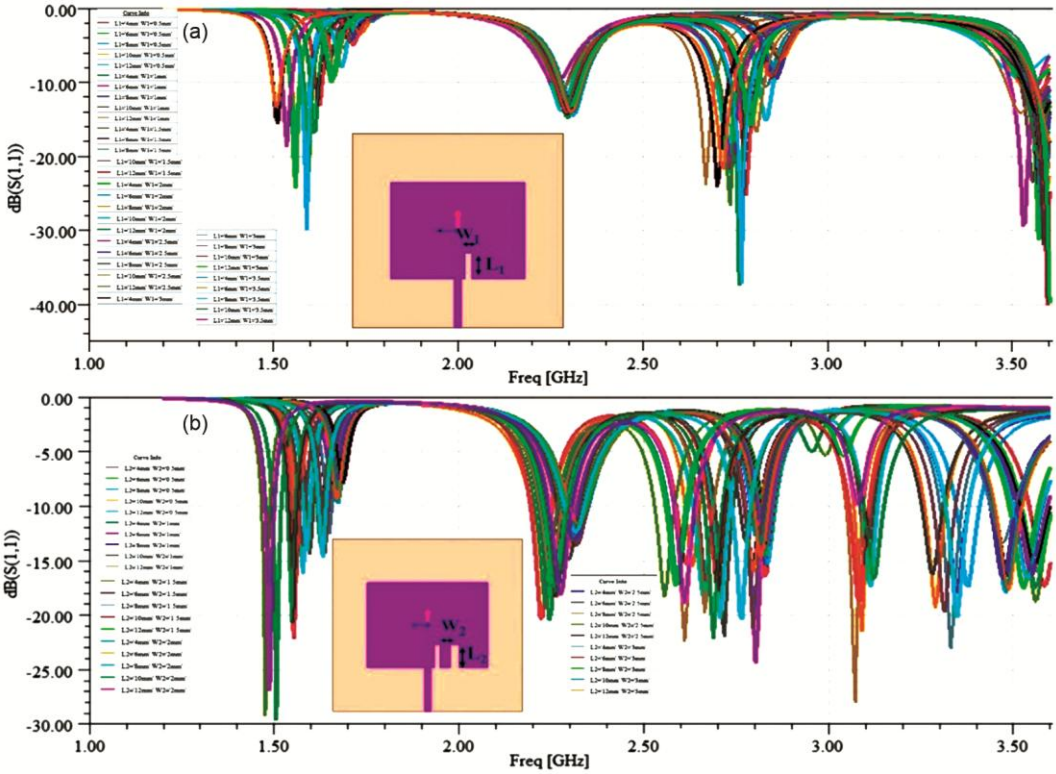

Fig. 2 — Parametric Analysis of Multiband Antenna (a) Effect of varying first slot width and length, and (b) Effect of varying second slot width and length

is placed near the first slot. Length (L_2) and width (W_2) of the second slot vary from 4 mm to 12 mm with a step size of 2 mm and 0.5 mm to 3.5 mm with a step size of 0.5 mm respectively. As depicted in Fig. 2 (b), for L_2 = 8 mm and W_2 = 3 mm the antenna exhibits resonance at four different operating bands with acceptable performance. The resulting multiband antenna structure shown in Fig. 1 (b) offers resonances at 1.64 GHz, 2.32 GHz, 2.8 GHz, and 3.3 GHz with a magnitude of S_{11} as -14.28 dB, -13.33 dB, -21.83 dB and -19.23 dB respectively. The simulated gains observed at the magnitudes observed at 1.64 GHz, 2.32 GHz, 2.8 GHz, and 3.3 GHz are 0.8 dB, 3.3 dB, 0.6 dB, and 0.1 dB respectively.

2.3 Miniaturized Multiband E-Slotted Rectangular Patch Antenna

To achieve miniaturization with improved performance, a metamaterial has been incorporated in the E-slotted multiband antenna design. In this design, a square shaped SRR of size 7 mm × 7 mm is designed. Permeability and permittivity of the unit cell are calculated using Eq (7) - Eq (10). The design geometry of the unit cell, its equivalent circuit, and its material characteristics are depicted in Fig. 3. The optimization of unit cell dimensions is done to realize negative permittivity and permeability in the operating frequency range. From Fig. 3 (d), the permeability, permittivity, impedance and refractive

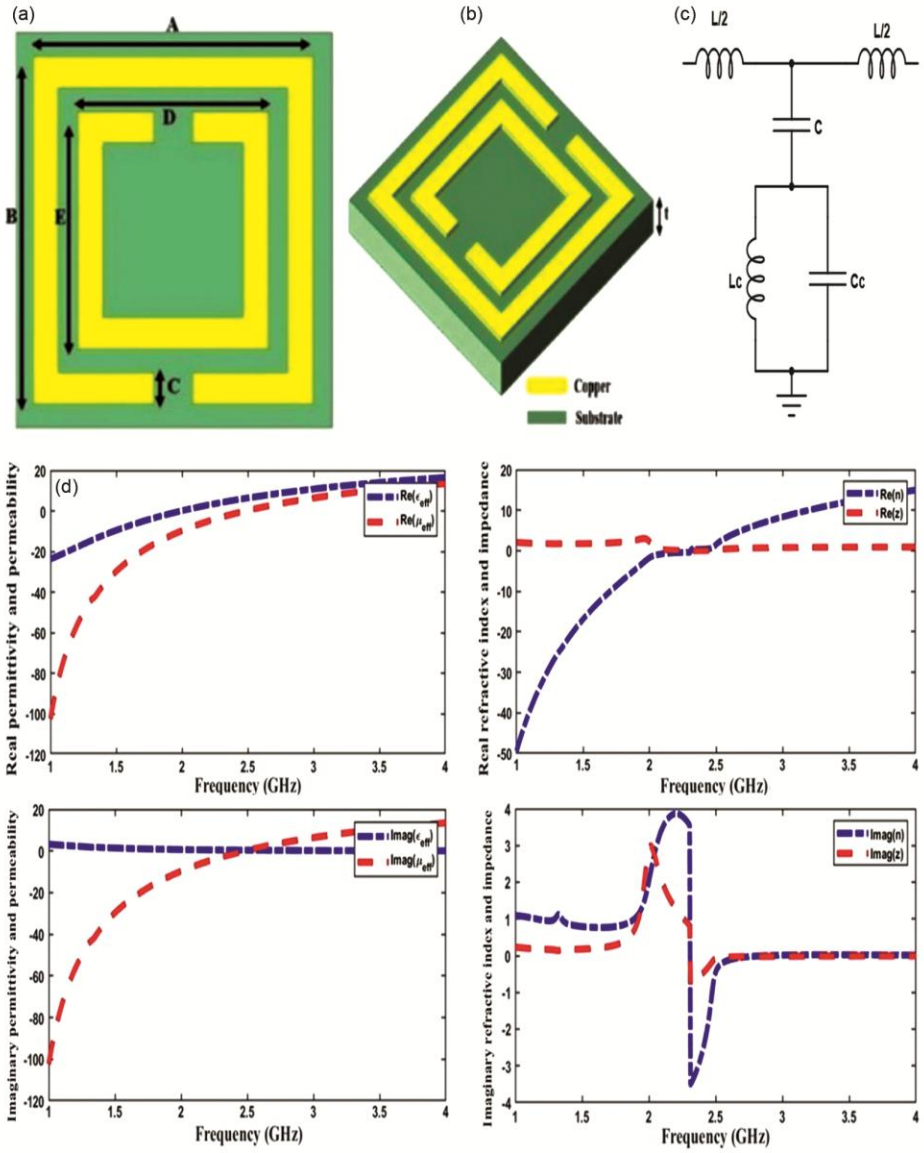

Fig. 3 — (a) Unit Cell dimensions of SRR / CSRR (b) Unit cell Structure (c) Equivalent Circuit, and (d) Permeability, Permittivity, Impedance and Refractive index

index of the unit cell are observed to be double negative. This implies the unit cell designed has left-handed material characteristics for the entire region of operation.

$$n_{eff} = \frac{1}{kd} cos^{-1}\left(\frac{1}{2*S_{21}}(1 - s_{11}^2 - s_{21}^2)\right) \quad \ldots (7)$$

$$Z_{eff} = \sqrt{\frac{(1+s_{11})^2 - s_{21}^2}{(1-s_{11})^2 - s_{21}^2}} \quad \ldots (8)$$

where, Z_{eff}, n_{eff} represents the effective impedance and refractive index of the designed unit cell, k represents the wave number, d denotes the thickness, S_{11} and S_{21} denote the reflection and transmission coefficient.

$$Permittivity = \frac{[re\ (n_{eff}) + j\ im\ (n_{eff})]}{[re\ (Z_{eff}) + j\ im\ (Z_{eff})]} \quad \ldots (9)$$

$$Permeability = [re\ (n_{eff}) + j\ im\ (n_{eff})] * [re\ (Z_{eff}) + j\ im\ (Z_{eff})] \quad \ldots (10)$$

In the process of miniaturization, a metamaterial unit cell is designed, and analyzed. The miniaturized multiband antenna structure with SRR and CSRR unit cells are given in Fig. 4 (a) and Fig. 4 (b), respectively. The modified design results in significant size reduction but there is a slight deviation in the resonating frequencies observed and are depicted in Fig. 4 (c). The inclusion of SRR resulted in low gain characteristics. On the other hand, the realized gains are observed to be positive and are in the acceptable range for the CSRR incorporated structure.

3 Results and Discussion

3.1 Simulated Results of Miniaturized Antenna with CSRR (Proposed Antenna)

A comparison of conventional patch antenna, E-slotted multiband antenna, and miniaturized multiband structure with SRR and CSRR is tabulated in Table 1. The optimized size-reduced patch antenna with CSRR structure has better radiation characteristics than the remaining structures as shown in Table 1. The overall size of the antenna before and after incorporation of meta material is 5760 mm ^{3} and 2700 m^3 respectively. When compared to the initial E slotted design, the miniaturized antenna with CSRR offers a size reduction of 53% as given in Eq. (11). Hence, the miniaturized antenna with CSRR structure is chosen as the final structure, and fabrication and validation of the antenna are done.

$$\%\ of\ Miniaturization = \frac{5760 - 2700}{5760} = 53\% \quad \ldots (11)$$

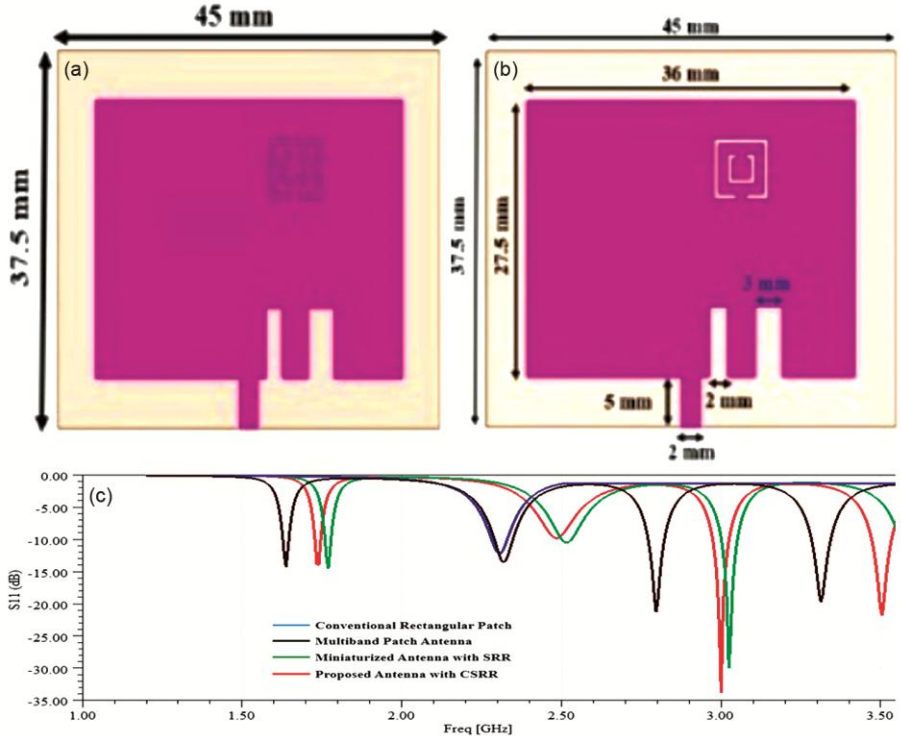

Fig. 4 — Miniaturized Multiband Antenna Structure (a) With SRR (b) With CSRR (Proposed Structure), and (c) Return Loss Plot

The simulation performance of the CSRR loaded multiband structure is discussed as follows. The S_{11} parameter indicates the reflected power by the load, a smaller value gives a better match. The proposed antenna radiates at four resonating frequencies 1.74 GHz, 2.48 GHz, 3 GHz, and 3.5 GHz with an S_{11} magnitude of -13.9 dB, -10.8 dB, -33.7 dB, and -21.81 dB respectively. Fig. 5 shows the simulated VSWR plot of the proposed antenna which is observed to be less than 2 at all the operating frequencies.

The 3D gain plot and E-field distribution for different operating frequencies are illustrated in Fig. 6 and Fig. 7, respectively. From the gain plot, it is observed that the gain at 1.74, 2.48, 3, and 3.5 GHz is 4.6 dB, 2.7 dB 4.7 dB, and 4.1 dB.

Table 1 — Radiation Characteristics

Antenna	Frequency (GHz)	S11 (dB)	Gain (dB)
Rectangular Patch	2.3	-12.28	3.1
	1.64	-14.28	0.8
E slotted Rectangular Patch	2.32	-13.33	3.3
	2.80	-21.83	0.6
	3.3	-19.2	0.1
	1.77	-14.5	2.9
Antenna with SRR unit cell	2.52	-11.3	2.7
	3.02	-30.0	-1.7
	3.59	-15.0	-1.9
	1.74	-13.9	4.6
Antenna with CSRR unit cell	2.48	-10.8	2.7
	3.0	-33.7	4.7
	3.50	-21.8	4.1

3.2 Fabrication and Validation of Proposed Antenna

The optimized size-reduced patch antenna incorporating a CSRR unit cell has been fabricated are presented in Fig. 8 (a) and (b). After fabricating, the antenna has been tested in an anechoic chamber with the measurement setup shown in Fig. 8 (c). The VNA measurement setup of the proposed antenna is depicted in Fig. 8 (d).

The measured radiation pattern of the proposed antenna at the resonating frequencies is depicted in Fig. 9. For 1.74 GHz and 2.48 GHz unidirectional patterns are observed. At 3 GHz and 3.5 GHz omnidirectional patterns are observed. The comparison graph for the simulated and measured S_{11} parameter is

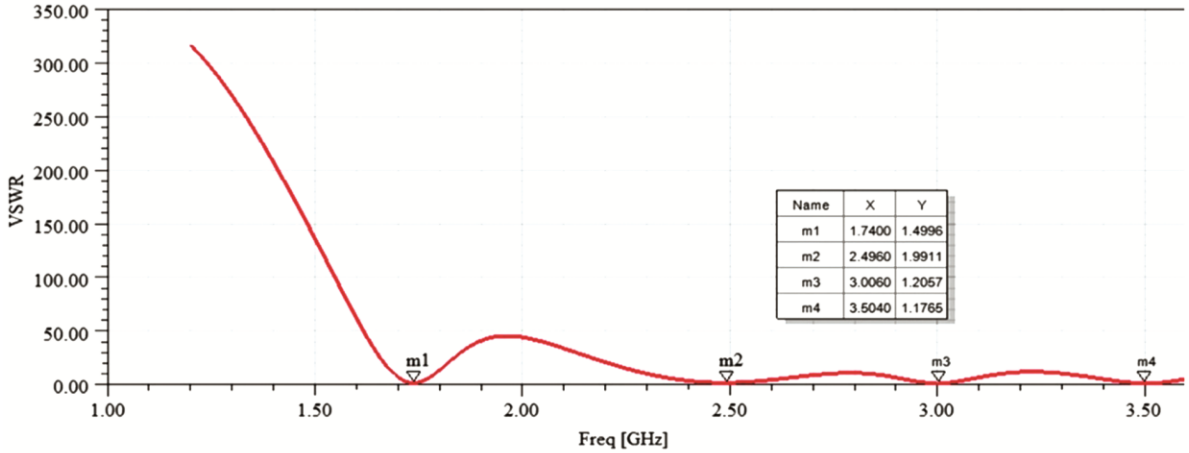

Fig. 5 — VSWR Plot of the Proposed Miniaturized Antenna with CSRR structure

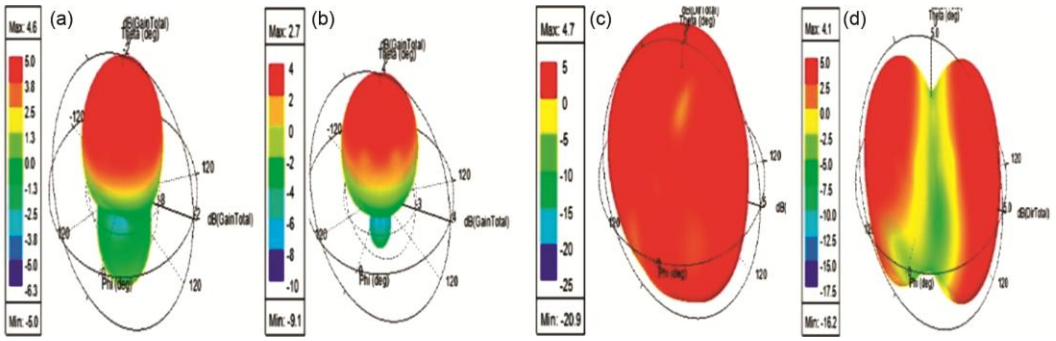

Fig. 6 — 3D plot- Gain at Resonating Frequencies (GHz) (a) 1.74 (b) 2.48 (c) 3, and (d) 3.5

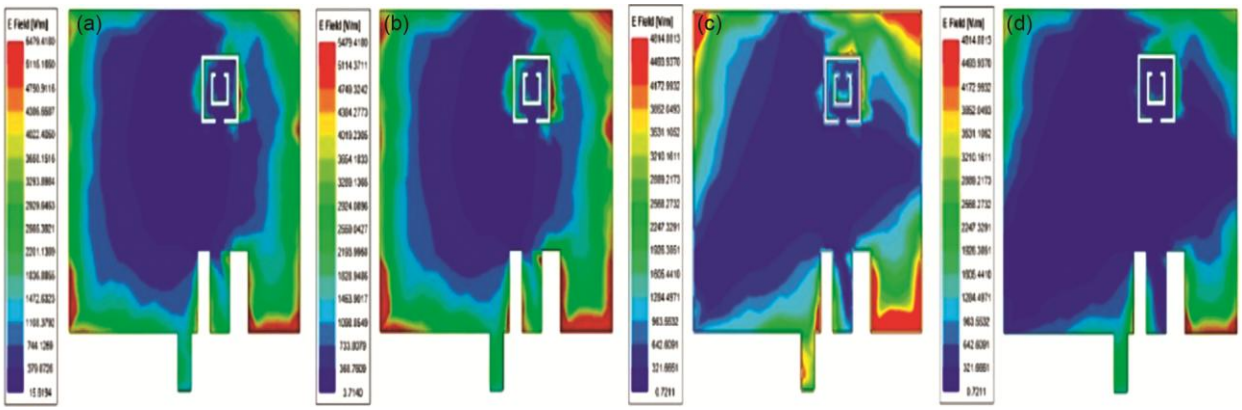

Fig. 7 — E-Field Distribution at Resonating Frequencies (GHz) (a) 1.74 (b) 2.48 (c) 3, and (d) 3.5

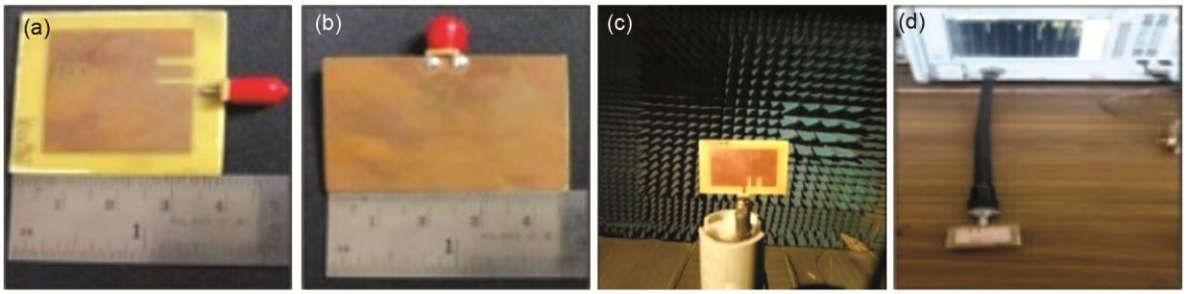

Fig. 8 — Fabricated Antenna (a) Front View (b) Bottom View (c) Anechoic Chamber - Inside View, and (d) VNA Measurement

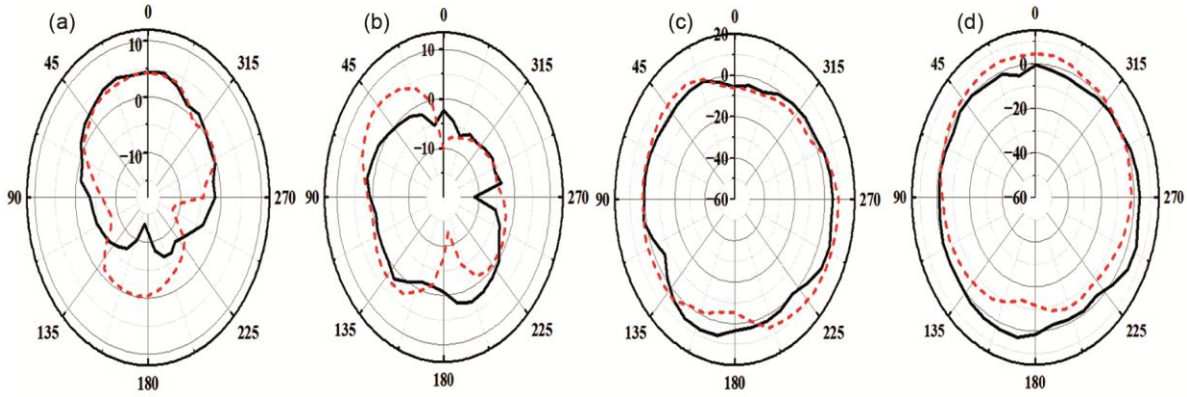

Fig. 9 — Measured E-Plane and H-Plane Pattern at Resonating Frequencies (a) 1.74 (b) 2.48 (c) 3, and (d) 3.5

presented in Fig. 10 and its performance across various metrics is summarized in Table 2.

The frequencies of the fabricated antenna are slightly varied from stimulated antenna results, but an appreciable S-parameter value is obtained for the frequency range. A comparative analysis of the proposed structure with the existing works on a FR4 substrate is given in Table 3. In comparison with existing works, the proposed work has a quad band operation with an average peak gain of 4.03 dB. Also in this work, both optimization algorithms and

Table 2 — Simulated and Measured Result Comparison

Results	f_r (GHz)	S_{11} (dB)	VSWR	Gain (dB)
Simulated	1.74	-13.98	1.49	4.6
	2.48	-10.8	1.99	2.7
	3.0	-33.7	1.20	4.7
	3.50	-21.81	1.17	4.1
Fabricated	1.74	-12.3	1.48	5.1
	2.49	-10.58	2	2.21
	2.98	-27.91	1.23	3.65
	3.49	-20.27	1.3	4.0

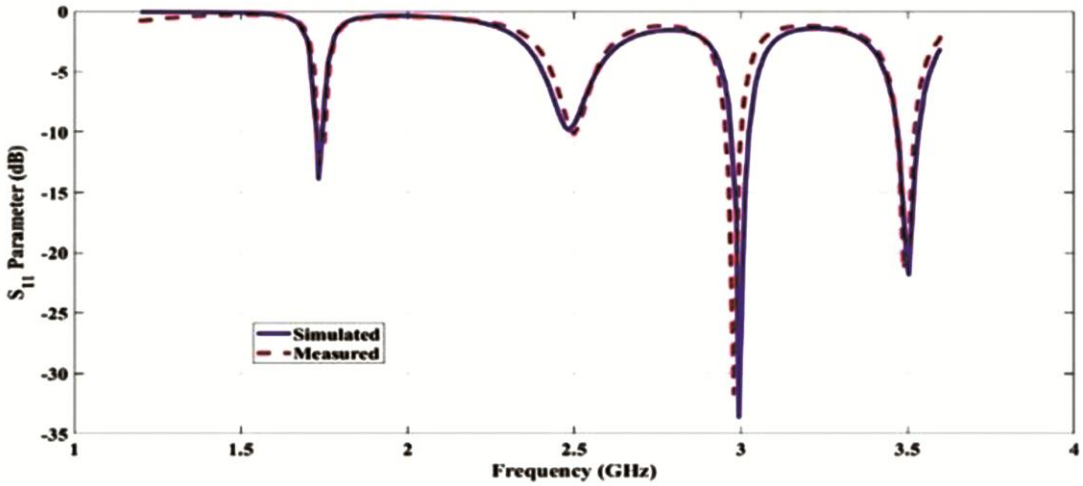

Fig. 10 — Simulated and Fabricated Results Comparison

Table 3 — Comparison with Existing Works

Ref.	Size (mm^3)	f_r (GHz)	S_{11} (dB)	Gain
[18]	42 x 32 x1.6	2.40	−28	1.63 dB
		5.03	−17	1.38 dB
		8.67	−22	2.95 dB
[19]	40 x 50 x 2	2.44	-25	35.0 dBi
		5.5	-40	3.53 dBi
[20]	25 x 16 x1.6	2.72	-24	0.72 dB
		4.58	-13	2.0 dB
[21]	33.6 x 36 ×1.6	2.40	-14	2.36 dB
[22]	20 x 20 x 1.6	3.21	-30	3.0 dBi
		3.60	-29	3.69 dBi
Proposed	37.5 x 45 x 1.6	1.74	-13.98	4.6 dB
		2.48	-10.8	2.7 dB
		3.0	-33.7	4.7 dB
		3.50	-21.81	4.1 dB

parameterization are deployed to determine the dimensions of the antenna and slots.

4 Conclusion

A multiband metamaterial inspired antenna for wireless applications is designed, simulated, and validated. In the initial structure, slots are introduced to attain multiband operation. For the miniaturization of the structure, both CSRR and SRR structure parameters have been analyzed. GA and QN algorithm analyses are performed to ensure the width of the proposed structure is at the optimal value. The geometry of the slots is determined using parametric analysis. The proposed antenna (multiband antenna with CSRR) has realized a size reduction of 53% in comparison with the conventional patch antenna. The proposed antenna operates in frequencies of 1.74 GHz (WiMax), 2.48 GHz (WLAN), 3 GHz (Internet of Things), and 3.5 GHz (5G) with efficient radiation. The array structure and meta surface implementation can be explored to improve the performance of the proposed antenna.

References

1 Valipour A, Kargozarfard M H, Rakhshi M, Yaghootian A & Sedighi H M, *Proc Inst Mech Engg Part L J Mater Des Appl*, 11 (2021) 236.

2 Geetanjali & Khanna R, *Indian J Sci Technol*, 10 (2018) 16.

3 Anusha K, *Int J Engg Adv Techno*, 8 (2018) 388.

4 Gollapalli A, P Sandeep Kumar, G Rokkesh, S Nithish, Vishal Hirawat & Rahul, *J Phys Conf Ser*, 62006 (2021).

5 Essid C, Chouikhi L, Mohammad A, Salah, Ben B & Sakli H, *Int J Adv Comput Sci Appl*, 15 (2024) 871.

6 David Ra M, Mohammad Saadh A W, Ali T & Kumar P, *Micromachines* 12 (2021).

7 Hidalgo A E & Rizo, *Ingeniare*, 27 (2019)22.

8 Sağık M, Altıntaş O, Ünal E, Özdemir E, Demirci M, Çolak Ş & Karaaslan M, *Wirel Pers Commun*, 118 (2021) 109.

9 Zou H, Zeng S, Li C & Ji J, *Eng Appl Artif Intell*, 138 (2024) 109381.

10 Fadamiro A O, Ntawangaheza J D, Famoriji O J, Zhang Z & Lin F, *IETE J Res*, 68 (2022) 1675.

11 Andrews C J M, Narayanan A S K & Marazhchal S, *Results Engg*, 24 (2024) 103269.

12 Marzouk M, *et al*., *Heliyon*, 1 (2024) e26087.

13 Geetharamani G & Aathmanesan T, *Wirel Pers Commun*, 113 (2020) 1331.

14 Bensid C, Bouknia M L, Sayad D, Elfergani I, Bendjedi H, Zegadi R, Rodriguez J, Varshney A, & Zebiri C, *Prog Electromagn Res C*, 139 (2024) .

15 Tariq S, Sethi W T, Rahim A A, Faisal F & Djerafi, *Sci Rep*,15 (2025) 1.

16 Pandya A, Upadhyaya T & Pandya K, *Prog Electromagn Res M*, 99 (2020) 03.
17 Haripriya K, Harini A S, Naveena M, Anusha K & Mohanageetha D, *8th International Conference on Advanced Computing and Communication Systems (ICACCS)*, 1 (2022) 1597.
18 Hasan M M, Faruq ue M R I & Islam M T, *Sci Rep*, 8 (2018) 1.
19 Wu X, Wen X, Yang J, Yang S & Xu J *IEEE Photonics J*, 14 (2022) 1.
20 Kumar R, Chandra A, Thummaluru S R, Khan M M & Chaudhary R K, *Int J Antennas Propag*, (2023) 2478853.
21 Pande S V & Patil D P, *Bull Electr Engg Informatics*, 13 (2024) 973.
22 Shobana M, *Alexandria Engg J*, 77 (2023) 351.